Dynamics of poly(ethylene oxide) in nanoscale confinements: A computer simulations perspective

V. Kuppa and E. Manias[a)]
Department of Materials Science and Engineering, The Pennsylvania State University, University Park, Pennsylvania 16802

(Received 3 September 2002; accepted 22 November 2002)

Molecular Dynamics simulations are used to explore the effect of severe −1 nanometer− confinement on the short-time dynamics of poly(ethylene oxide) (PEO). Bulk and intercalated systems have been atomistically modeled to comparatively illustrate their differences. In particular, we aim to trace the molecular level mechanisms responsible for the counter intuitive distribution of relaxation times recorded by solid state ^{2}H NMR for the C−H bond reorientations in confinements. Computer simulations complement the experiments and reveal that factors such as local density inhomogeneities, proximity of Li^+, and disorder in the system, combine to determine the PEO segmental dynamics. In contrast with the respective bulk PEO systems, where a clear transition from distinct solid to liquid like dynamics takes place with increasing temperatures, for the nanoscopically confined chains there persists a coexistence of fast and slow segmental relaxations over the same temperature range. © *2003 American Institute of Physics.*
[DOI: 10.1063/1.1538601]

I. INTRODUCTION

Polymers intercalated in layered-inorganic compounds such as graphite, 2:1 aluminosilicates, and transition metal halides have recently attracted very strong interest, both as novel composite materials, as well as model systems for nanoscopically confined polymers. Experimental[1,2] and simulation approaches[3–8] offer a detailed molecular description of the behavior of these systems, and a very striking picture is emerging for the physics of polymers in *nm*-scale confinements. These systems self-assemble in highly-ordered intercalated structures, which allow for the preparation of samples with macroscopic quantities of nanoscopically-confined polymers. Thus, conventional analytical techniques can be employed to probe nanometer thin polymer layers, revealing the segmental dynamics of polymers in severe confinements between solid surfaces. Examples of such studies include solid state NMR, dielectric spectroscopy, x-ray and neutron techniques.[9–16] In addition, molecular modeling approaches have proved useful in complementing the experimental techniques.

Together, experimental and molecular modeling studies of intercalated polymers have unveiled a very unexpected picture for the structure and dynamics of polymers in nanoscopic confinements. Even for the simplest systems, such as those of a 1 *nm* thin poly(ethylene oxide) (PEO)/Li^+ film confined between solid surfaces,[9–13] an understanding of the segmental relaxations, chain dynamics, or even the Li^+ motion has yet to be satisfactorily completed.[13] The current opinion is that PEO arranges in the interlayer gallery in an amorphous bilayer parallel to the confining surfaces,[14] with Li cations located in the immediate vicinity of the solid surfaces,[15] a picture which is supported by experimental findings and also by simulations.[3] This structural description challenges the traditional viewpoint, which assumed extended crystalline PEO chain conformations with the Li cations located in the center of the films.[10,17] Beyond the structure of these films, the segmental dynamics in confinement, as probed by solid state NMR, also reveal features that defy the intuitively expected polymer behavior. In contrast to the expected ''dead'' layer with all of its segmental dynamics being suppressed by the extreme—two monomers thin—confinement, NMR records a remarkably rich behavior with fast relaxing segments existing even at such low temperatures where the bulk PEO has a completely solidlike response.[9,12]

Although NMR provides a detailed picture of the segmental dynamics, it cannot reveal the molecular origins responsible for them. In order to investigate the underlying physics behind the experimentally observed phenomena, we performed Molecular Dynamics computer simulations to directly observe the atomistic motions investigated by NMR. Towards this goal, we employed an atomistically explicit model for the intercalated system, which mimics poly(ethylene oxide) confined between montmorillonite (MMT) layers, and we specifically focus on the short time (tens of ns) reorientation dynamics of the monomers.

II. MOLECULAR DYNAMICS SIMULATION DETAILS

Molecular Dynamics (MD) simulations are employed to comparatively study the short time (ns) dynamics of nanoscopically confined and bulk PEO systems, focusing on exploring how the confinement affects the segmental dynamics of PEO. Two different force fields developed for earlier simulations of Li^+/bulk PEO by Müller–Plathe[18] and Smith *et al.*,[19,20] were evaluated in our confined geometries, where the interactions with the montmorillonite sheets are modeled after those used by Hackett *et al.*[3] Both sets of parameters reproduce well the structure of the bulk PEO/Li^+ systems

a)Author to whom correspondence should be addressed; electronic mail: manias@psu.edu

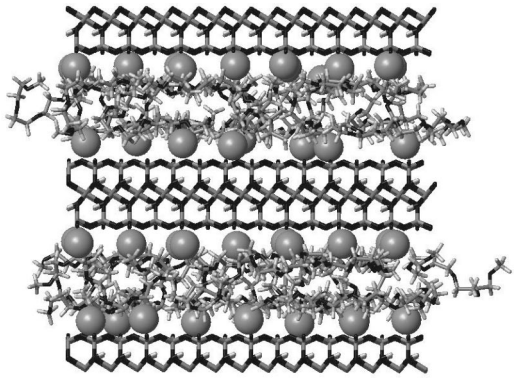

FIG. 1. Schematic of the simulation box with double slit geometry. Li^+ ions are represented by their van der Waals spheres, so as to clearly show their positions with respect to the inorganic walls.

and of the confined PEO/MMT systems, as observed experimentally. However, the latter force field—by Smith[19,20]—reproduces more accurately some of the important dynamic details in the the Li^+/PEO and the Li^+/PEO/MMT systems. Specifically, using that force-field:[19,20] (a) The Li^+ diffusion coefficients trace well the experimental values, both in bulk PEO and in PEO/MMT intercalates, whereas the force field by Müller–Plathe overestimates the experimental Li cation diffusivities by an order of magnitude, both in bulk PEO[21] and in PEO/MMT intercalates;[22] (b) the distance where the Li^+ is trapped on the silicate surfaces—exhibiting lengthy time periods of vibration around an equilibrium position[22]—is accurately reproduced at 0.45 *nm* from the center of the silicate layer, in quantitative agreement with NMR studies.[15] The detailed force-field employed in the present work, including both the PEO and the MMT parameters, is given elsewhere.[22]

Due to the existence of a net charge in the silicate platelets and the neutralizing Li^+, as well as high partial charges of the PEO chains, the electrostatics determine the system behavior to a large extent. Thus, it becomes imperative to obtain an accurate calculation of the coulombic forces, which faithfully reproduces the response of the real systems. To this end, we evaluated various techniques[23] for estimating the long range electrostatic interactions, and the generalized reaction field (GRF) method proved to be the most accurate and fast method for these highly charged systems.[24] For the GRF calculations an effective dielectric constant of 3.0 was used beyond a cutoff distance of 1.0 *nm*.

For our confined systems, simulations were performed at constant *NVT*. Periodic boundary conditions were employed in all three directions, with a box size of $3.696\times3.656\times3.558$ *nm* containing two montmorillonite surfaces parallel to the *xy* plane (Fig. 1). The spacing between the MMT surfaces was chosen to match the experimental systems, which self assemble in an extremely well-defined superstructure of 0.80 *nm* thin PEO films,[13] and the number of PEO and Li^+ atoms were chosen to agree with the experimental values of organic density and Li^+ surface density. Our simulation box defines two PEO/Li^+ films intercalated between two inorganic layers, as shown in Fig. 1, with 23 PEO hexamers and 21 Li^+ in each confined film. This ''double slit'' geometry was chosen as it allows for more accurate electrostatic calculations.[25]

For the bulk, constant NPT simulations were performed in a manner similar to those described in Refs. 19, 20, with a cutoff radius of 0.9 *nm* and a distance dependent dielectric constant.[26] Pressure and temperature were stabilized by a weak coupling to their reference values, via the Berendsen method.[27] Simulations of the bulk were carried out at six temperatures (273, 298, 323, 373, 398 and 423 K) paralleling the NMR studies. The initial simulation box size was chosen so as to match the PEO density to the experimental data[28] at each temperature. All simulation boxes contained 8 Li^+I^- units solvated by 69 PEO hexamers. Periodic boundary conditions were employed in all three directions.

The time step in all simulations was 1 *fs* (a time interval that is adequate for capturing local polymer dynamics, as well as lithium motion). After energy minimization, initial equilibration MD runs of 10 *ns* were performed for all temperatures, followed by productive runs of 2 to 6 *ns*, depending on temperature.

III. RESULTS AND DISCUSSION

A. Dynamic inhomogeneities

Focusing on the short term (*ns*) dynamics in our confined systems, our aim is to complement the experimental NMR studies and provide insights on the relevant molecular scale processes underlying the local segmental dynamics in nanoconfined poly(ethylene oxide). On the outset, we would like to mention the experimental behavior for which we are trying to provide a molecular level explanation. NMR findings[15] have reported the simultaneous existence of fast (relaxation times of a few *ns*) and slow (relaxation times in the μs range) C–^{2}H bond reorientational dynamics for PEO restricted in 0.8 *nm* wide films, i.e., the size of ca. two PEO monomers. Moreover, deuterium line shapes were obtained for bulk and intercalated systems across a wide range of temperatures, starting below T_g and reaching above the melting point of the bulk polymer.[12] The bulk PEO displays line shapes which are characteristic of classic solid to liquid transition in the system dynamics. At temperatures below the Tg for the bulk system, segmental motions are highly suppressed and the ^{2}H lines display sharp features reminiscent of textbook examples of solid behavior, indicative of no C–^{2}H bond decorrelation. With increasing temperature, the C–^{2}H bonds start to explore more orientations in space, leading to a decrease in signal intensity of the two solid peaks and the build up of an averaged central peak. At even higher temperature, above the melting point, liquidlike dynamics are completely established, as is evident from the presence of an extremely sharp, single-peaked ^{2}H line, indicative of fast and complete C–^{2}H bond reorientational decorrelation.[12]

In contrast to the rather straightforward behavior of the bulk PEO line shapes, the ^{2}H NMR lines obtained from the intercalated PEO reveal a much more complex behavior:[12] At the lower temperatures studied, the ^{2}H line has two peaks corresponding to a solid phase, but there is also a perceptible loss of spectral definition, illustrating the presence of small

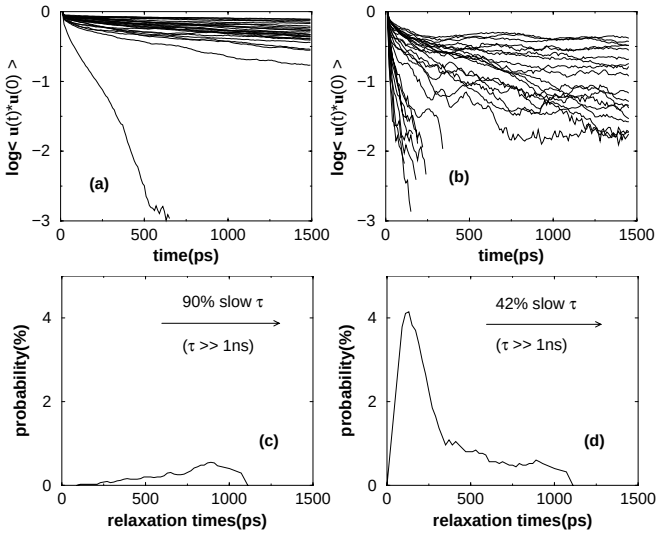

FIG. 2. The C–H bond vector time autocorrelation functions at 273 K of a *few typical* C–H bonds for bulk PEO/Li^+ system (a), and nanoscopically confined system (b). The corresponding distributions of relaxation times for *all* the C–H bond vectors are shown in (c) for the bulk and in (d) for the confined systems.

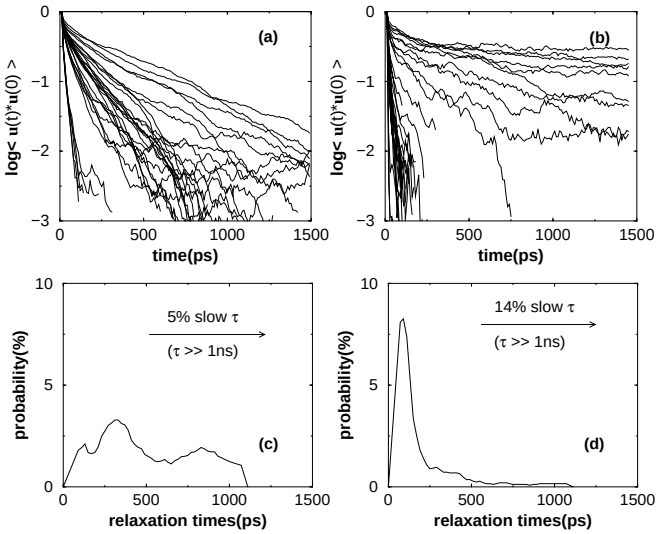

FIG. 3. The C–H bond vector time autocorrelation functions at 423 K of a *few typical* C–H bonds for bulk PEO/Li^+ system (a), and nanoscopically confined system (b). The corresponding distributions of relaxation times for *all* the C–H bond vectors are shown in (c) for the bulk and in (d) for the confined systems.

amplitude dynamics. As the temperature is raised, there is a narrowing of the dual-peak solidlike signal and an increase in signal intensity at the center of the ^{2}H line, corresponding to an increased ability of the C–^{2}H bonds to reorient in space. This behavior persists for a wide range of temperatures—above and below the bulk melting point—denoting a distinct coexistence of solidlike and liquidlike dynamics. At the highest temperature studied, where the solid dual-peak disappears, there exists a marked width to the central peak indicating that, despite the high temperature, the system does not exhibit complete C–^{2}H bond reorientation.

In order to compare against the NMR experiments, we modeled both intercalated and bulk Li^+/PEO systems over the experimental temperature range.[12] In these MD simulations the dynamics of entities can be directly followed through the time-trajectory of the particles. In accordance with the NMR experiments, we monitor the C–H bond reorientational relaxations as a measure of the local segmental dynamics. In particular, we define and follow the time autocorrelation functions (ACF) of the C–H bond, which effectively measures the same temporal relaxation as the NMR studies.

The ACF of the C–H bond vector ($\mathbf{v}$) is defined by

$$\mathrm{ACF}(\delta t) = \frac{\mathbf{v}(t_o+\delta t)\cdot\mathbf{v}(t_0)}{|\mathbf{v}(t_0)|^2}, \tag{1}$$

where δt is the time elapsed after the reference time t_o, with multiple time origins (t_o) selected uniformly across the simulated trajectories to obtain better statistics. The physical significance of the ACF being to follow the time evolution of the C–H bond vector by quantifying how much time elapses until the initial orientation is ''forgotten.'' In Figs. 2 and 3 we show the log of the ACFs of a few typical C–H bond vectors for bulk [Figs. 2(a), 3(a)] and confined [Figs. 2(b), 3(b)] systems, for the lowest and highest temperatures simulated (273 and 423 K, respectively). The corresponding distributions of relaxations times calculated for *all* the C–H bonds in the systems (both bulk and confined) are shown in Figs. 2(c), 2(d) and Figs. 3(c), 3(d). It is evident that our simulations capture the essential behavior of the bulk and confined system dynamics, as seen experimentally in the NMR, even though we focus on a much shorter time scale than what the NMR probes (fast relaxing species are defined as those whose ACFs decrease to e^{-1} of their initial value within 1 *ns*, and slow species are those which show no marked reorientation during the duration of the simulation, 2–6 *ns*). We do see that the bulk has a much more homogeneous dynamical behavior than the confined systems, with characteristic solidlike and liquidlike dynamics seen for the lowest and highest temperatures. The confined systems exhibit a more wide distribution of dynamic responses, even at these two extreme temperatures (in concert with the NMR results); at the highest and lowest temperature marked populations of the confined PEO's C–H bonds are characterized by fast reorientation for the lowest T [more than 50% of the C–H population at 273 K, Fig. 2(d)], but also very slow (solidlike) motions for the highest T [14% of the C–H population at 423 K, Fig. 3(d)]. This occurs only for the confined PEO systems and is a significant departure from the behavior of the bulk PEO [at 273 K less than 8% of the C–H population exhibits fast relaxations, and at 423 K about 5% relaxes at times longer than 1 *ns*, Figs. 2(c)–3(c), both being below the NMR detection, typically requiring ca. 10% of the probed nuclei]. The focus of this study is to trace the molecular mechanisms responsible for this behavior in the confined geometries, and from this standpoint we shall continue the rest of the paper.

B. Molecular origins

In order to quantify the above discussion on the dynamics of confined PEO, we analyzed closely the correlations between the rate of reorientation of the C–H bond vectors

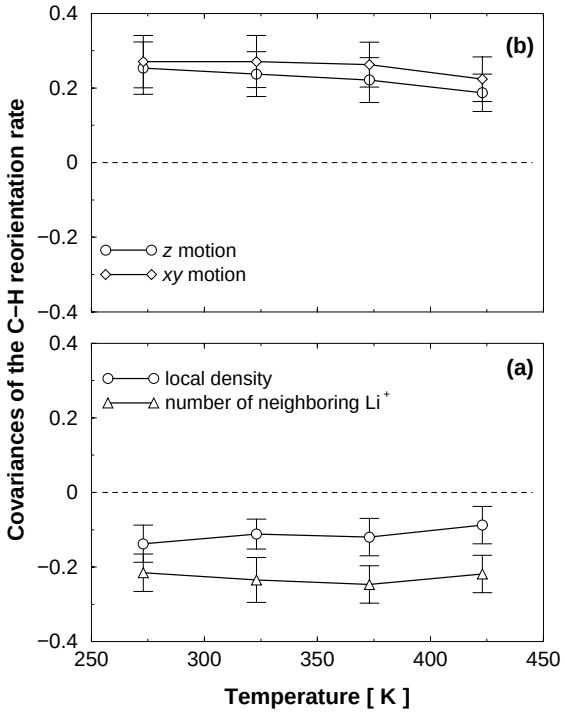

FIG. 4. (a) Covariances of the C–H reorientation rate with local density around the C–H bond and with the number of proximal Li^+ ions. (b) Covariances of the C–H bond reorientation rate with translational motion of the respective carbon, both in the z direction and in the xy plane.

and the various factors that could possibly have an effect on it. This was realized through the definition of the covariance between two variables:

$$\mathrm{cov}(\delta\phi,X)\equiv\frac{\langle(\delta\phi-\langle\delta\phi\rangle)\cdot(X-\langle X\rangle)\rangle}{\sqrt{\sigma^2(\delta\phi)\sigma^2(X)}}, \tag{2}$$

where $\delta\phi$ is the rate of change of the bond direction vector for C–H, $\langle\delta\phi\rangle$ is the ensemble average of $\delta\phi$, X is the factor whose effect on the reorientation we wish to measure and $\langle X\rangle$ is the ensemble average of X. $\sigma^2(\delta\phi)$ and $\sigma^2(X)$ are the corresponding ensemble variances, of $\delta\phi$ and X, respectively. Using this equation, we estimated the influence of different physical mechanisms on the reorientation behavior of the C–H in the confined system (Fig. 4). In our study, instead of using relaxation times from the bond vectors ACFs as a measure of local segmental dynamics,[4] we studied the rate of change of the direction of C–H bond vectors ($\delta\phi = \mathrm{d}\phi/\mathrm{d}t|_{t_o}$, i.e., the instantaneous velocity associated with the C–H directional change). This approach was selected because many C–H moieties show complex behavior over the trajectory time, undergoing time periods of fast and slow dynamics over the course of the simulation run, thus making it difficult to define a single relaxation time for their dynamics. As will become obvious later, this occurs because the local environment around these bonds, which greatly influences their dynamics, is continuously changing.

Earlier simulation studies of polystyrene in similar confined, intercalated geometries have shown that the local segmental relaxations are *strongly* coupled to local density variations in the confined film.[4] Probing the same correlation here for the PEO systems, i.e., the covariance of the rotational relaxation of a C–H bond versus the local density around this C–H bond [Fig. 4(a)], we also see a definite connection between the two. Specifically, this covariance is negative across all temperatures, denoting that the rate of bond vector reorientation is *faster* for C–H bonds located in regions of *lower* local density, in agreement with the polystyrene behavior.[4] However, the low absolute value of the covariance suggests that there must exist more factors which contribute to the dynamical behavior of PEO in confinement.

Another correlation investigated, probably the simplest one conceptually, is the covariance correlating the translational displacement of C–H bonds to their reorientation behavior. We explored two different covariances in this context, connecting C–H reorientations to translations parallel to the confining surfaces, i.e., in the xy plane, and perpendicular to them, i.e., in the z direction. Translations were quantified through the instantaneous displacement in the respective direction (i.e., $\mathrm{d}z/\mathrm{d}t|_{t_o}$ and $\mathrm{d}\sqrt{x^2+y^2}/\mathrm{d}t|_{t_o}$). As seen in Fig. 4(b), there is a positive correlation between translational motions of the C–H bonds and their rotations. This means that the *greater* the motion of the C–H bond, the *faster* the rate of reorientation of the corresponding bonds. This behavior is not unexpected, since polymer segments that move in space are also more likely to undergo rotation around the carbons, as part of the polymer backbone flexing and trans-gauche isomerizations. For our simulation box geometry, motions in the z direction correspond to adsorption/desorption events of C–H moieties, which intuitively are expected to contribute the most to the C–H rotational relaxation. However, the covariances of the C–H reorientation with the z and xy motions are comparable, which means that motions in the plane parallel to the walls are as important for the C–H reorientation as are the adsorption/desorption events.

Perhaps the most interesting covariance identified is the one between the reorientation rate of the C–H bond vectors and the number of Li^+ close to that C–H bond. The negative value of this covariance suggests that the *larger* the number of Li^+ located close to a bond, the *slower* its rate of reorientation is. The explanation for such an observation is not immediately evident; this behavior arises from the characteristic arrangement of the PEO chains and Li^+ cations in the slit pore. It is known, both from earlier simulations[3] and NMR spin lattice relaxations studies,[15] that the lithium cations reside in close proximity to the wall surfaces, due to the strong electrostatic attraction to the negatively charged silicate layers. The PEO chains are arranged primarily parallel to the walls, with multiple oxygens coordinated to the Li^+ cations.[3] This materials arrangement effectively allows the Li^+ cations, which are strongly coupled to the wall surfaces,[22] to mediate an indirect anchoring of the PEO chains to the solid surfaces. Consequently, the greater the number of lithiums close to a particular C–H bond, the greater is the indirect anchoring of that chain fragment to the solid surface. In this manner, reduced mobility is imposed on the chain fragments which are coordinated to lithiums, which also leads to a lower rate of reorientation for the C–H bonds. This hindrance to motion—implicitly reflected in the negative value seen in our covariance—can be also directly seen in close observation of the system trajectories,

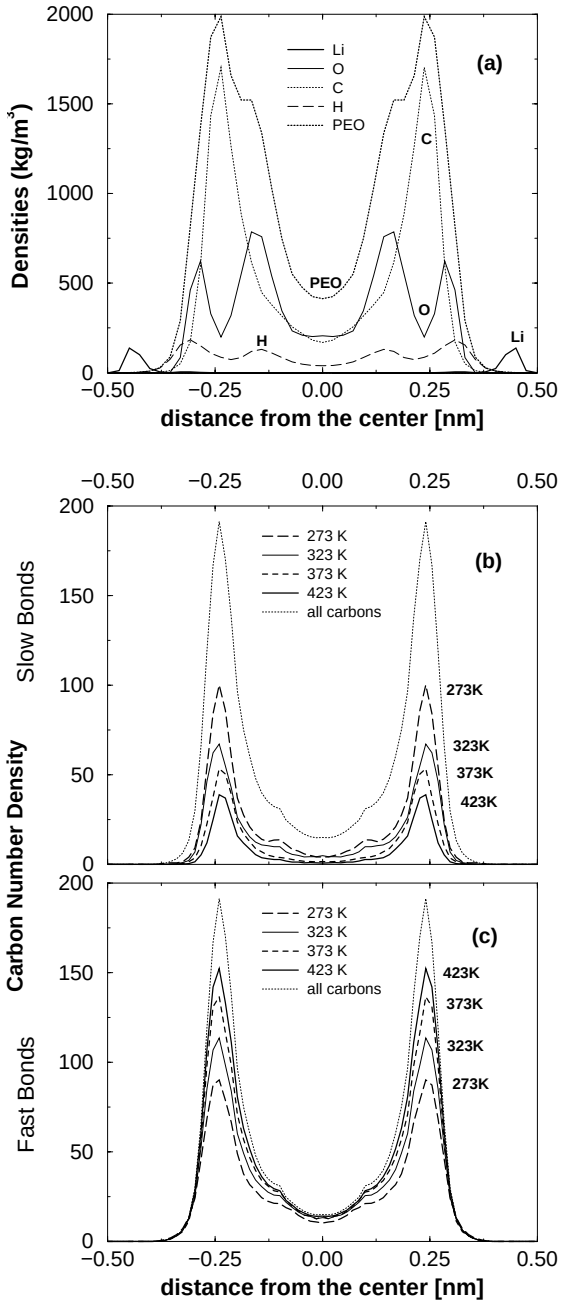

FIG. 5. (a) Density profiles of the various atom types in the simulation cell, with the center of the slit pore at 0.0. Number density profiles for carbons belonging to "slow" relaxing C–H bonds (b) and "fast" relaxing C–H bonds (c), at different temperatures.

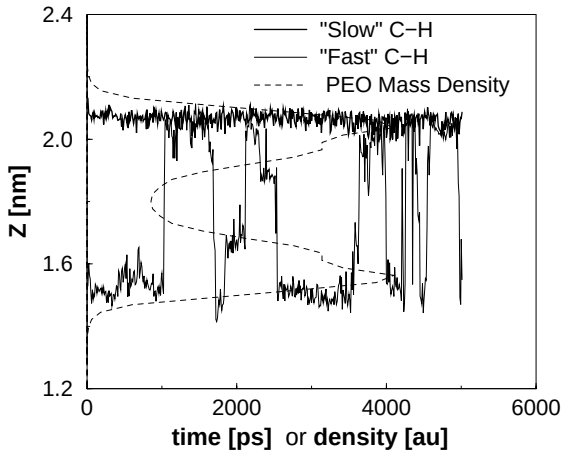

FIG. 6. z-projection of 5 ns trajectories of representative slow and fast relaxing carbon atoms, superimposed on the density profile of the total PEO mass density across the slit pore.

for all the simulated temperatures (an example to this is given later in Fig. 6).

To provide further insight into the effects of confinement on the dynamics of the polymer, we also studied the distribution of various species across the slit pores, seen in Fig. 5(a). Of special importance are the distributions of carbon atoms that correspond to slow and fast reorientation rates of C–H bond vectors. For much wider confined films, slow relaxing moieties and chains are located in the vicinity of the confining surfaces and fast relaxing ones are located in the center of the slit.[29] However, for our systems—which can be considered as bilayers—it is seen [Figs. 5(b) and 5(c)] that the distributions for both slow and fast carbon atoms follow the same basic pattern as the total carbon density profile across the slit; i.e., they are arranged in a bilayer structure with two peaks corresponding to the PEO layer near each confining surface [Fig. 5(a)]. This behavior denotes that both fast and slow entities display similar distributions across the confined film, with no overwhelming spatial preference of the slow moieties next to the walls, as is the case in wider confined films.[29]

A closer examination of the density profiles shows that in the center of the slit, and independent of temperature, there exist more fast relaxing carbon atoms than slow ones. This effect can be understood by looking back to the covariances calculated before. First, the local density in the center of the slit is typically lower than near the walls; given the negative covariance between the rate of reorientation and the local density, more fast species are expected to exist in the center of the slit. Second, the Li^+ spend most of their time close to the walls and very seldom are they found in the center of the slit;[3,22] given the negative covariance between the reorientation rate and the number of lithiums close to the C–H bonds, more slower relaxing moieties are expected in the physisorbed layers on each wall, where Li^+ cations hinder their motion and reorientation. An illustration of this latter effect can be seen in Fig. 6, where the short time z trajectories of two carbons are plotted, belonging to a slow and a fast C–H bond. The carbon of the slow C–H bond is pinned on the surface due to coordinations of Li^+ to its neighboring oxygens. The carbon of the fast C–H undergoes a number of desorption/adsorption instances on both confining surfaces, while in between them it translates through the center of the confined film. Often, this translation is also accompanied by reorientation of the C–H bond vector. With increasing temperature there is an increase in the number of adsorption/ desorption instances (per time), as well as an accompanying increase in the reorientation rate of the C–H bond. All these factors give rise to an increase of the fast population in the center of the film with temperature, as well as a decrease of the slow population next to the surfaces with temperature [Figs. 5(b) and 5(c)].

Beyond these quantitative changes in the populations of

"fast" and "slow" C–H bonds in the confined films, there appears no distinct behavioral change with temperature (as is the case with the bulk PEO, Figs. 2, 3, and 5). In order to better understand the origins of this behavior we compared the structural details of the PEO chains in the bulk and the confined PEO chains.

C. Structural details

The segmental dynamics of the simulated bulk PEO change qualitatively as the temperature crosses the melting point of the poly(ethylene oxide) (ca. 323 K). Although our oligomer chains are too short to capture the genuine crystalline behavior of PEO polymers, there do exist some structural changes that take place at about 323 K. These changes manifest themselves both in the chain conformations (Appendix), as well as the ordering of the chain molecules. Differences between the ordering of the bulk and the confined chains provide clues about the confinement induced dynamics in our simulated systems.

In order to quantify the ordering of the chain molecules at different temperatures, we employ two different parameters that measure the orientational and translational order in the systems. The parameter of translational order (τ) is defined by

$$\tau_i = \frac{\int_0^{\xi_c} |g_i(\xi) - 1| d\xi}{\xi_c}, \tag{3}$$

where ξ is the normalized radial distance between carbon atoms ($\xi = r\rho^{1/3}$, where r is the carbon radial distance, and ρ is the carbon number density); $g_i(\xi)$ is the interchain radial distribution function (rdf) around the ith carbon in the simulation cell; ξ_c is a cutoff distance, whose maximum value is determined by the size of the simulation box. In our case, for both the bulk and the confined systems, the cutoff was chosen as half of the smallest box dimension [after this distance, $g_i(r)$ go to 1, so further counting is meaningless since the integrands vanish]. In a first approximation, τ_i is a measure of the periodic separation/spacing in the vicinity of the ith carbon, when considering all interchain carbons in the confined film. Values for τ_i vary between 0 and 1, with lower values reflecting no preferential spacing and higher values indicating a tendency towards crystallinity.

In our study, we examined the stacking periodicity for each of the carbons (τ_i) in the PEO chains. Such an analysis results in a *distribution* of translational order parameters for the system carbons, for each different simulation temperature, for bulk and confined systems as shown in Fig. 7. The mean value, τ is obtained by the ensemble average of the individual τ_i distribution ($\langle \tau_i \rangle$), or equivalently[30] by the equation:

$$\tau = \frac{\int_0^{\xi_c} |g(\xi) - 1| d\xi}{\xi_c}, \tag{4}$$

where $g(\xi)$ is now the total interchain carbon–carbon radial distribution function for the whole system.[30,31] $\langle \tau_i \rangle$ is thus a scalar parameter indicative of the stacking periodicity between adjacent chains for the whole system. This same parameter was used in a recent computer simulation study of water.[30] Values for $\langle \tau_i \rangle$ also vary between 0 and 1, with lower values reflecting no preferential spacing in the system (zero corresponds to an ideal gas[30]) and higher values indicating a higher system crystallinity (one would be a perfect crystal structure[30]).

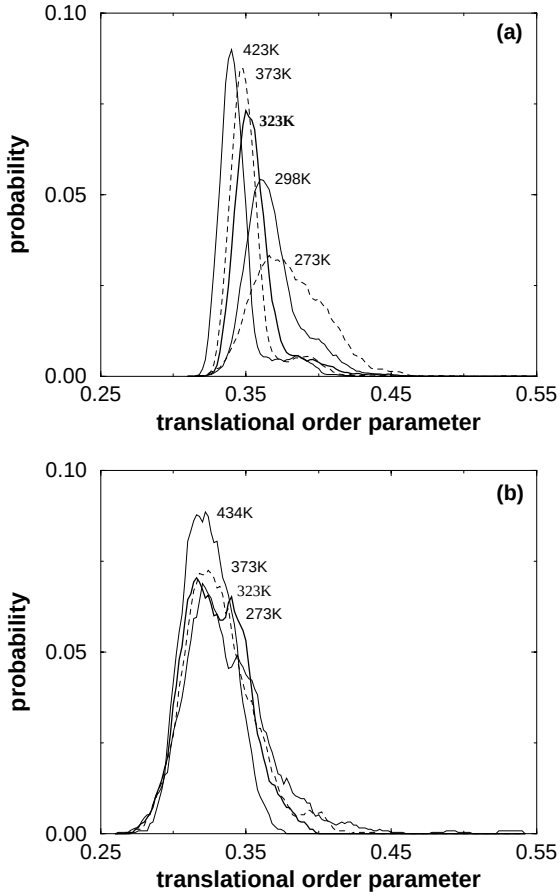

FIG. 7. Parameter of translational order distributions for carbon atoms in bulk PEO (a) and in the confined systems (b).

For the bulk systems, $\langle \tau_i \rangle$ decreases with temperature, indicating that as the temperature is raised the tendency for the oligomers to orient in a crystalline fashion decreases [Fig. 7(a)]. Moreover, the distribution becomes narrower as temperature increases, since regions of periodic packing (low-τ_i peak) disappear and the system becomes disordered throughout. For the confined system there is no marked change in the order parameter $\langle \tau_i \rangle$ with temperature, albeit a small change in the width of the distribution [Fig. 7(b)]. Comparing the translational order parameters for the bulk and confined systems we see that for the confined chains $\langle \tau_i \rangle$ is lower than the bulk value (independent of temperature). This difference in $\langle \tau_i \rangle$ indicates that the spatial order in the confined system is reduced as compared to the bulk polymer, despite the "ordering" effect imposed by the confining solid surfaces. Furthermore, the confined systems appear more disordered than the bulk systems for all temperatures simulated, even when compared with the bulk at the highest temperature.

In order to complete the comparison of the chain arrangements in the bulk and the confined systems we also quantified the orientational order in the systems. The param-

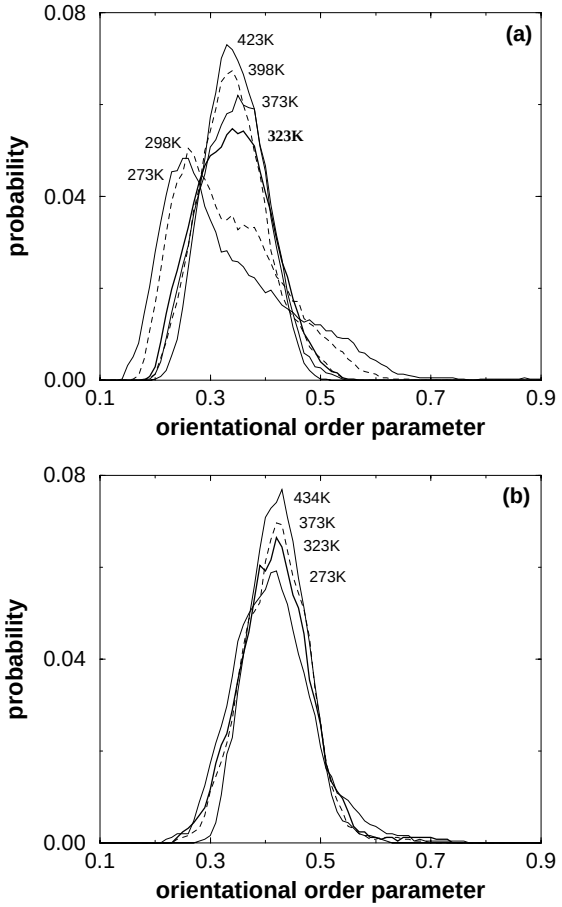

FIG. 8. Parameter of orientational order distributions for oxygen atoms in bulk PEO (a) and in the confined systems (b).

eter of orientational order (q) is defined in the same spirit as the translational order parameter, following the definitions by[31]

$$q_i = \frac{3}{32}\sum_{j=1}^{3}\sum_{k=j+1}^{4}\left(\cos\psi_{j,i,k}+\frac{1}{3}\right)^2, \tag{5}$$

where $\psi_{j,i,k}$ scans all the angles centered on the ith oxygen atom and defined by all pairs (j,k) of its four nearest interchain oxygen neighbors. The numerical factors used normalize the value for q_i between 0 and 1 (with zero corresponding to a perfect tetrahedral arrangement centered around the i oxygen[32]). In a first approximation, $\langle q_i\rangle$ quantifies how much the orientation of four nearest interchain oxygens deviates from a tetrahedron arrangement.[33] Thus, from the definition of q_i through Eq. (5), low $\langle q_i\rangle$ values indicate an orientation close to a tetrahedral structure, larger values correspond to increasing disorder, and $\langle q_i\rangle = 1$ corresponds to a completely random oxygen orientation.

Both in the bulk and confined systems, the parameter of orientational order q_i was calculated by considering the angles defined by each oxygen i and its four nearest interchain oxygen neighbors (i.e., four nearest oxygens not belonging to the same chain). For the bulk system [Fig. 8(a)] $\langle q_i\rangle$ increases with temperature, with a marked change in the mean value and the distribution of q_i at 323 K. This means that the PEO oxygen atoms tend to lose orientational order with increasing temperature, with a distinct change in orientational order at ca. 323 K. For the confined chains [Fig. 8(b)] the $\langle q_i\rangle$ values are systematically higher than the bulk values, independent of temperature; thus, as with the translational order, the confined systems are more orientationally disordered than the bulk, even when compared to the bulk PEO at the highest temperature simulated. Moreover, the q_i distribution for the confined PEO is markedly insensitive to temperature [Fig. 8(b)], suggesting that the orientational disorder remains at the same level throughout the temperatures studied [much like the translational order in these same systems, Fig. 7(b)].

Comparing the parameters of order—translational and orientational—between the bulk and nanoscopically confined chains, it becomes clear that the confined chains are more disordered than any of the bulk systems, despite the parallel conformations imposed by the solid walls. This probably is a result of the large numbers of Li^+ cations near the surfaces which are coordinated to the PEO oxygens, thus promoting highly disordered (''crown''-like) conformations.[3] Moreover, there is no marked temperature dependence of the structural order for the confined systems, in contrast with the behavior of the bulk equivalents; this is in concert with the insensitivity of the segmental dynamics on the temperature, which remain qualitatively the same for the confined chains across all temperatures studied.

IV. CONCLUSIONS

Molecular dynamics simulations were used to study the physics of poly(ethylene oxide) oligomers in severe confinement. Focusing on short time scales (few *ns*), we were able to draw parallels with and capture the response observed by solid state NMR in similar systems. Namely, a coexistence of fast and slow relaxation times was observed for the nanoscopically confined chains, over a wide temperature range. In our efforts to trace the molecular origins of these confinement induced segmental dynamics, we identified several relevant mechanisms: Translations, local density variations, and proximity of coordinated Li^+ cations were connected to the dynamical inhomogeneities observed in the confined systems. Fast relaxing C–H segments are primarily present in regions of low local density and no/few coordinated lithiums; whereas lithium coordination to the ethylene oxide groups resulted in anchoring chains on the confining walls, inducing solidlike segmental dynamics even at high temperatures. Finally, the structural order in the confined systems was found to be smaller than the corresponding bulk, and insensitive to temperature in the simulated range (273–423 K). This happens despite the orientational effect of the confining walls to the confined chains, and is tentatively attributed to the chain coordination with the lithiums in the system.

ACKNOWLEDGMENTS

This work was partially supported by the ACS/PRF (PRF Grant No. 37274-G5) and the Penn State MRSEC (NSF/DMR 0080019). Additional support of V.K. by NIST/FRD (DoC Grant No. 60NANB1D0066), and of E.M. from

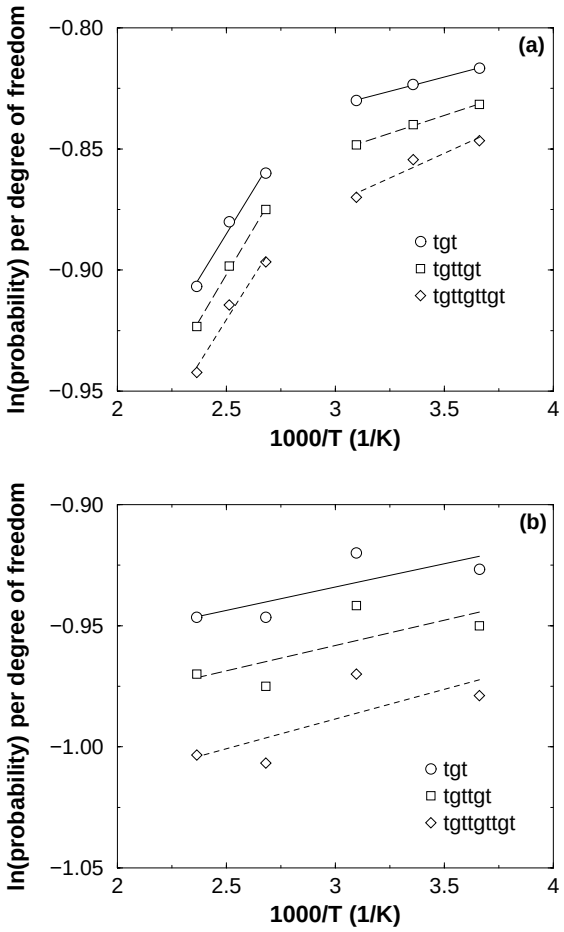

FIG. 9. Normalized probabilities of "crystalline" dihedral sequences: triads (tgt), hexads ($tgttgt$), and enneads ($tgttgttgt$). The probabilities are enumerated by the simulations and are plotted versus inverse temperature, (a) for bulk PEO, and (b) for nanoscopically confined PEO.

Different conformations of dihedral angles along the chain backbones can be identified and each dihedral can be assigned either a trans (t) or a gauche (g) state. In crystalline PEO, backbone dihedrals adopt a trans state for C–O bonds and gauche for the C–C bonds, resulting in crystallizable helical chain conformations.[34] In our study, sequences of dihedrals were studied for the three segment lengths: triads (with a crystallizable conformation of tgt), hexads ($tgttgt$), and enneads ($tgttgttgt$); the results were normalized by the degrees of freedom in each case and were compared between the bulk and the nanoscopically confined systems. Probabilities of specific sequences at each temperature were enumerated by directly counting the sequences' occurrence in the simulation ensemble. Figure 9(a) shows the probabilities of the crystallizable dihedral sequences (i.e., tgt, $tgttgt$, and $tgttgttgt$) in the bulk PEO systems. For all the three kinds of sequences, there is a decrease in the probability with increasing temperature, following the Boltzmann temperature dependence. In addition, for the bulk system, there is a sharp change in the slopes of the sequence probabilities, somewhere in the range of 323 K–373 K. A similar analysis for the confined PEO chains [Fig. 9(b)] shows that, unlike the bulk, the slope of the probability versus $1/T$ does not display any sharp change. In connection with our prior discussion of the parameters of translational and orientational order, the analysis of the chain configurations strongly suggests that for our bulk PEO chains there is some crystallization taking place at low temperatures, which melts as T is increased above 323–373 K. In contrast, for the nanoscopically confined systems we observe a disordered structure throughout the simulated T-range, despite the geometrical constraints and the orientational effects imposed by the confining surfaces.

the "Virginia S. and Philip L. Walker, Jr." endowment is also thankfully acknowledged. We would also like to express our gratitude to D.B. Zax (Cornell University) for useful discussions and for sharing their NMR results prior to publication.

APPENDIX: PEO CHAIN CONFORMATIONS IN BULK AND CONFINEMENT

In an earlier investigation of lithium dynamics,[22] in bulk and confined PEO systems identical to those studied here, we saw a sharp change of the Li^+ diffusion in bulk PEO (following two different VFT lines on either side of the PEO melting point temperature). However, the Li^+ diffusion in the confined systems showed no sharp change across the same temperature range (273–423 K), and followed a single VFT thermalization throughout. Those findings parallel our observations here on the segmental dynamics of the PEO chains. Although our chain molecules $[H-(CH_2-O-CH_2)_6-H]$ are too short to reproduce the genuine crystallization behavior of PEO polymers, there are indications supporting a change of behavior ("transition") at a temperature quite close to the melting point of bulk PEO. Traces of this change are found in the structural order of these systems, i.e., in the interchain packing and ordering. Additional traces are also found in the chain conformations.

[1] E. P. Giannelis, R. K. Krishnamoorti, and E. Manias, Adv. Polym. Sci. **138**, 107 (1999).
[2] M. Alexandre and P. Dubois, Mater. Sci. Eng., R. **28**, 1 (2000).
[3] E. Hackett, E. Manias, and E. P. Giannelis, Chem. Mater. **12**, 2161 (2000).
[4] E. Manias, V. Kuppa, D.-K. Yang, and D. B. Zax, Colloids Surf., A **187**, 509 (2001).
[5] R. F. Loring, J. Chem. Phys. **106**, 701 (1997).
[6] J. Y. Lee, A. R. C. Baljon, and R. F. Loring, J. Chem. Phys. **109**, 10321 (1998).
[7] A. R. C. Baljon, J. Y. Lee, and R. F. Loring, J. Chem. Phys. **111**, 9068 (1999).
[8] J. Y. Lee, A. R. C. Baljon, and R. F. Loring, J. Chem. Phys. **111**, 9754 (1999).
[9] R. A. Vaia, B. B. Sauer, O. K. Tse, and E. P. Giannelis, J. Polym. Sci., Part B: Polym. Phys. **35**, 59 (1997).
[10] P. Aranda and E. Ruiz-Hutsky, Chem. Mater. **4**, 1395 (1992).
[11] L. Wang, M. Rocci-Lane, P. Brazis, C. R. Kannewurf, Y. Kim, W. Lee, J. Choy, and M. G. Kanatzidis, J. Am. Chem. Soc. **122**, 6629 (2000).
[12] S. Wong, R. A. Vaia, E. P. Giannelis, and D. B. Zax, Solid State Ionics **86**, 547 (1996).
[13] R. A. Vaia, S. Vasudevan, W. Krawiec, L. G. Scanlon, and E. P. Giannelis, Adv. Mater. **7**, 154 (1995).
[14] R. K. Krishnamoorti (private communication).
[15] D. K. Yang and D. B. Zax, J. Chem. Phys. **110**, 5325 (1999).
[16] S. Anastasiadis, K. Karatasos, G. Vlachos, E. Giannelis, and E. Manias, Phys. Rev. Lett. **84**, 915 (2000).
[17] B. K. G. Theng, *Formation and Properties of Clay Polymer Complexes* (Elsevier, New York, 1979).
[18] F. Muller-Plathe, Acta Polym. **45**, 259 (1994).
[19] G. D. Smith, R. L. Jaffe, and D. Y. Yoon, J. Phys. Chem. **97**, 12752 (1993).

[20] G. D. Smith, R. L. Jaffe, and D. Y. Yoon, J. Am. Chem. Soc. **117**, 530 (1995).
[21] F. Muller-Plathe and W. F. van Gunsteren, J. Chem. Phys. **103**, 4745 (1995).
[22] V. Kuppa and E. Manias, Chem. Mater. **14**, 2171 (2002).
[23] For the long range electrostatic interactions we have applied and compared Ewald sums, the particle-particle particle-mesh (PPPM) method, and the generalized reaction field (GRF) method. The PPPM and GRF methods were comparable in accuracy, however, the PPPM was much more computationally expensive. For these charged systems, the Ewald sums were proven quite inaccurate, probably due to an unrealistic periodicity of strong dipoles, as repeated through the periodic boundary conditions.
[24] I. G. Torini, R. Sperb, P. E. Smith, and W. F. van Gunsteren, J. Chem. Phys. **102**, 5451 (1995).
[25] M. Chávez-Páez, K. Van Workum, L. de Pablo, and J. J. de Pablo, J. Chem. Phys. **114**, 1405 (2001).
[26] J. D. Londano, B. K. Annis, A. Habenschuss, O. Borodin, G. D. Smith, J. Z. Turner, and A. K. Soper, Macromolecules **30**, 7151 (1997).
[27] H. J. C. Berendsen, J. P. M. Postma, W. F. van Gunsteren, A. DiNola, and J. R. Haak, J. Chem. Phys. **81**, 3684 (1984).
[28] G. D. Smith, D. Y. Yoon, R. L. Jaffe, R. H. Colby, R. Krishnamoorti, and L. J. Fetters, Macromolecules **29**, 3462 (1996).
[29] I. Bitsanis and P. Pan, J. Chem. Phys. **99**, 5520 (1993).
[30] J. R. Errington and P. G. Debenedetti, Nature (London) **409**, 318 (2001).
[31] P. L. Chau and A. J. Hardwick, Mol. Phys. **93**, 511 (1998).
[32] If an oxygen is located at the center of a regular tetrahedron whose vertices are occupied by its four nearest neighbours, cos $\psi_{j,i,k}=-1/3$. Thus, in a perfect tetrahedral network, $q_i=0$. If, on the other hand, the mutual arrangement of oxygens is random, as in molecules of an ideal gas, the six angles associated with the central oxygen are independent, and $\langle q_i\rangle=1$ (Ref. 31).
[33] A different choice of symmetry (other than tetrahedral) would only change the numerical factors in Eq. (5) and the x-axis in Fig. 8, but would not change the relative differences between the bulk and the confined systems (Refs. 30, 31).
[34] S. Neyertz, D. Brown, and J. O. Thomas, J. Chem. Phys. **101**, 10064 (1994).